



Published in final edited form as:

Am J Surg Pathol. 2015 July ; 39(7): 957–967. doi:10.1097/PAS.0000000000000404.

Molecular Characterization of Inflammatory Myofibroblastic Tumors with Frequent *ALK* and *ROS1* Fusions and Rare Novel *RET* Gene Rearrangement

Cristina R Antonescu^{1,*}, Albert JH Suurmeijer², Lei Zhang¹, Yun-Shao Sung¹, Achim A Jungbluth¹, William D Travis¹, Hikmat Al-Ahmadie¹, Christopher DM Fletcher^{*,3}, and Rita Alaggio^{*,4}

¹Department of Pathology, Memorial Sloan Kettering Cancer Center, New York, NY ²Department of Pathology, University Medical Center Groningen, University of Groningen, Groningen, Netherlands ³Department of Pathology, Brigham and Women's Hospital, Boston, MA

⁴Department of Pathology, University of Padova, Padova, Italy

Abstract

Approximately 50% of conventional IMTs harbor *ALK* gene rearrangement and overexpress ALK. Recently gene fusions involving other kinases have been implicated in the pathogenesis of IMT, including *ROS1* and in one patient *PDGFRB*. However, it remains uncertain if the emerging genotypes correlate with clinicopathologic characteristics of IMT. In this study we expand the molecular investigation of IMT in a large cohort of different clinical presentations and analyze for potential genotype-phenotype associations. Criteria for inclusion in the study were typical morphology and tissue availability for molecular studies. The lack of ALK immunoreactivity was not an excluding factor. As overlapping gene fusions involving actionable kinases are emerging in both IMT and lung cancer, we set out to evaluate abnormalities in *ALK*, *ROS1*, *PDGFRB*, *NTRK1* and *RET* by FISH. Additionally, next generation paired-end RNA sequencing and FusionSeq algorithm was applied in 4 cases, which identified *EML4-ALK* fusions in 2 cases. Of the 62 IMTs (25 children and 37 adults), 35 (56%) showed *ALK* gene rearrangement. Of note, *EML4-ALK* inversion was noted in 7 (20%) cases, seen mainly in the lung and soft tissue of young children including 2 lesions from newborns. There were 6 (10%) *ROS1* rearranged IMTs, all except one presenting in children, mainly in the lung and intra-abdominal and showed a distinctive fascicular growth of spindle cells with long cell processes, often positive for ROS1 IHC. Two of the cases showed *TFG-ROS1* fusions. Interestingly, one adult IMT revealed a *RET* gene rearrangement, a previously unreported finding. Our results show that 42/62 (68%) of IMTs are characterized by kinase fusions, offering a rationale for targeted therapeutic strategies. Interestingly 90% of fusion negative IMT were seen in adults, while >90% of pediatric IMT showed gene rearrangements. *EML4-ALK* inversion and *ROS1* fusions emerge as common fusion abnormalities in IMT, closely recapitulating the pattern seen in lung cancer.

*Correspondence to: Cristina R Antonescu, MD, Department of Pathology, Memorial Sloan Kettering Cancer Center, 1275 York Ave, New York, NY 10065 (antonesc@mskcc.org); Christopher D.M. Fletcher, Department of Pathology, Brigham and Women's Hospital, Boston, MA (cfletcher@partners.org) and Rita Alaggio, University of Padova, Padova, Italy (rita.alaggio@gmail.com).

Conflict of interest: none

INTRODUCTION

Inflammatory myofibroblastic tumor (IMT) is a distinctive neoplasm composed of myofibroblastic-type cells intimately associated with a lymphoplasmacytic inflammatory infiltrate. IMTs can occur ubiquitously at any anatomic site, but show a predilection for lung, soft tissue and viscera of children and young adults. Based on its potential for local recurrence and rare metastases, IMT is classified as a mesenchymal neoplasm of intermediate biological potential¹. Approximately half of the IMTs harbor a clonal translocation that activates the anaplastic lymphoma kinase (ALK)-receptor tyrosine kinase gene located at 2p23 locus². As a result ALK protein is overexpressed and can be detected at the immunohistochemical level, being used as a reliable diagnostic marker for this disease. ALK is a receptor-type protein tyrosine kinase, which is rendered oncogenic either as a result of a gene fusion, such as in anaplastic large cell lymphoma, lung cancer and IMT, or due to a missense mutation as seen in neuroblastoma and anaplastic thyroid cancer. In IMT, multiple fusion partners to *ALK* have been described, including *TPM3*, *TPM4*, *RANBP2*, *TFG*, etc, which most likely contribute a strong promoter to the fusion transcript²⁻⁵.

IMTs display a wide morphologic spectrum, ranging from an inflammatory ‘pseudotumor’ with predominant hyalinization and chronic inflammation and only a paucity of lesional spindle cells, to a highly cellular myofibroblastic proliferation and occasionally frankly sarcomatous neoplasm, lacking significant inflammatory or/and fibromyxoid stromal component. Due to its markedly variable phenotype and lack of objective immunoprofile, the diagnosis of ALK-negative IMTs has been often a diagnosis of exclusion and regarded as a potential waste-basket of different entities, including reactive/inflammatory processes, such as the fibro-inflammatory IgG4 related disease⁶, idiopathic retroperitoneal fibrosis⁷, and at the other end of the spectrum, the so-called inflammatory fibrosarcoma. Thus the lack of recurrent genetic abnormalities outside the *ALK* gene rearrangements played a significant drawback in accurate classification of these tumors. Furthermore, ALK immunoreactivity, as an expression of *ALK*-based gene fusions, is more prevalent in pediatric IMT compared to the adult counterpart^{3, 8, 9}. However, it remains unclear if this discrepant prevalence of ALK abnormalities is an intrinsic difference in biology of IMT between the two age groups, or instead is merely a reflection of a wider spectrum of lesions present in adults that are classified under the broad term of IMT, which otherwise have no genetic relationship. Generally pathologic features of IMT do not correlate well with behavior¹⁰. However, the epithelioid variant of IMT, which shows distinctive nuclear membrane or perinuclear ALK immunostaining pattern, has been associated with a more aggressive clinical outcome¹¹. In a subset of these lesions a *RANBP2-ALK* fusion has been detected by RT-PCR. Furthermore, until very recently there was limited knowledge about the pathogenesis of the remaining half of IMTs lacking ALK expression. In this regard, in a seminal study using next generation sequencing, 6 of 9 ALK-negative IMT tumors showed the presence of fusions in either *ALK*, *ROS1* or *PDGFRB*, suggesting that IMT is largely a kinase fusion-driven neoplasm¹². The study was initiated by the dramatic response to the ROS1 inhibitor crizotinib in an index case of a treatment-refractory ALK negative IMT pediatric patient. In this study we investigate abnormalities of a wide variety of actionable kinases in a large series of pediatric

and adult IMT, encompassing a broad range of clinical presentations to further elucidate their pathogenetic mechanisms and potential correlations with morphology.

MATERIAL AND METHODS

Tumor Samples and Patient Information

The Pathology files and the personal consultation files of the senior authors (CRA, WT, CDF, RA) were searched for the diagnosis of IMT. Slides were re-reviewed and cases were included in the study if showing a typical morphologic appearance. Tumors were evaluated for their morphologic appearance (spindle, epithelioid), degree of nuclear pleomorphism (mild, moderate), amount of inflammatory component (brisk, scarce), type (myxoid, fibrous) and amount (prominent, scant) of stroma. ALK immunostaining was reviewed in all cases, however, the lack of ALK immunoreactivity was not an excluding factor. All cases were tested with ALK01 (Ventana Ready to use) and 3 cases were additionally tested with D5F3 (Cell Signaling; 1:50). *ROS1*-rearranged IMTs were then tested with ROS1 antibody (Cell Signaling; clone D4D6; 1:25). Immunostains for SMA, desmin and myogenin were also reviewed in all cases. None of the ALK-negative tumors showing an immunoprofile in keeping with smooth or skeletal muscle differentiation were included in the study. In fact only 3 pediatric tumors showed desmin positivity in the absence of myogenin reactivity, two of them showing *ALK* gene rearrangement and one *ROS1* rearrangement. In fact only The study was approved by the Institutional Review Board 02-060.

Fluorescence In Situ Hybridization (FISH)

FISH on interphase nuclei from paraffin-embedded 4-micron sections was performed applying custom probes using bacterial artificial chromosomes (BAC), covering and flanking genes that were identified as potential fusion partners in the RNA-seq experiment. BAC clones were chosen according to UCSC genome browser (<http://genome.ucsc.edu>), see Supplementary Table 1. The BAC clones were obtained from BACPAC sources of Children's Hospital of Oakland Research Institute (CHORI)(Oakland, CA)(<http://bacpac.chori.org>). DNA from individual BACs was isolated according to the manufacturer's instructions, labeled with different fluorochromes in a nick translation reaction, denatured, and hybridized to pretreated slides. Slides were then incubated, washed, and mounted with DAPI in an antifade solution, as previously described¹³. The genomic location of each BAC set was verified by hybridizing them to normal metaphase chromosomes. Two hundred successive nuclei were examined using a Zeiss fluorescence microscope (Zeiss Axioplan, Oberkochen, Germany), controlled by Isis 5 software (Metasystems, Newton, MA). A positive score was interpreted when at least 20% of the nuclei showed a break-apart signal. Nuclei with incomplete set of signals were omitted from the score. All cases were tested for *ALK* gene rearrangements. Tumors lacking *ALK* gene abnormalities were further investigated by FISH for changes in *ROS1*, *PDGFRB*, *NTRK1* and *RET*. *ALK* positive tumors were further investigated by *EML4* abnormalities by FISH and *ROS1*-rearranged IMT were tested for *TFG* alterations.

RNA Sequencing and Data Analysis by FusionSeq—Four cases were analyzed by RNA sequencing. Total RNA was prepared for RNA sequencing in accordance with the

standard Illumina mRNA sample preparation protocol (Illumina). Briefly, mRNA was isolated with oligo(dT) magnetic beads from total RNA (10 µg) extracted from case. The mRNA was fragmented by incubation at 94°C for 2.5 min in fragmentation buffer (Illumina). To reduce the inclusion of artifactual chimeric transcripts due to random priming of transcript fragments into the sequencing library because of inefficient A-tailing reactions that lead to self ligation of blunt-ended template molecules¹⁴, an additional gel size-selection step was introduced prior to the adapter ligation step. The adaptor-ligated library was then enriched by PCR for 15 cycles and purified. The library was sized and quantified using DNA1000 kit (Agilent) on an Agilent 2100 Bioanalyzer according to the manufacturer's instructions. Paired-end RNA-sequencing at read lengths of 50 or 51 bp was performed with the HiSeq 2000 (Illumina).

All reads were independently aligned with the CASAVA 1.8 software provided by Illumina against the human genome sequence (hg19) and a splice junction library, simultaneously. The splice junction library was generated by considering all possible junctions between exons of each transcript. We considered the University of California, Santa Cruz (UCSC) Known Genes annotation set¹⁵ to generate this library via RSEQtools, a computational method for processing RNA-seq data¹⁶. The mapped reads were converted into Mapped Read Format¹⁶ and analyzed with FusionSeq¹⁷ to identify potential fusion transcripts. FusionSeq is a computational method successfully applied to paired-end RNA-seq experiments for the identification of chimeric transcripts¹⁸⁻²⁰. Briefly, paired-end reads mapped to different genes are first used to identify potential chimeric candidates. A cascade of filters, each taking into account different sources of noise in RNA-sequencing experiments, was then applied to remove spurious fusion transcript candidates. Once a confident list of fusion candidates was generated, they were ranked with several statistics to prioritize the experimental validation. In these cases, we used the DASPER score (Difference between the observed and Analytically calculated expected SPER): a higher DASPER score indicated a greater likelihood that the fusion candidate was authentic and did not occur randomly.

Reverse Transcription Polymerase Chain Reaction (RT-PCR)

An aliquot of the RNA extracted above from frozen tissue (Trizol Reagent; Invitrogen; Grand Island, NY) was used to confirm the fusion transcript identified by FusionSeq. RNA quality was determined by Eukaryote Total RNA Nano Assay and cDNA quality was tested for PGK housekeeping gene (247 bp amplified product). Three microgram of total RNA was used for cDNA synthesis by SuperScript® III First-Strand Synthesis Kit (Invitrogen, Carlsbad, CA). RT-PCR was performed using the Advantage-2 PCR kit (Clontech, Mountain View, CA) for 30 cycles at a 64.5°C annealing temperature. Primers used were: EML4_exon2: 5'-AAGATCATGTGGCCTCAGTG-3' and ALK_exon 20: 5'-AGCTTGCTCAGCTTGTACTC-3', as previously described²¹. Amplified products were purified and sequenced by Sanger method.

RESULTS

62 IMT tumors were selected based on typical morphologic features and WHO pathologic criteria¹ as well as availability of tissue for molecular and immunohistochemical studies. An effort was made to include a wide variety of anatomic locations and ages at presentation. Microscopically, the cohort also covered a broad spectrum of morphologies, spanning from a hypocellular proliferation with hyalinized and prominent chronic inflammatory component, reminiscent of the so-called 'inflammatory pseudo-tumor', to a highly cellular spindle or epithelioid neoplasm with minimal inflammation or stroma. As only half of the IMT reported in the literature show ALK immunoexpression, the lack of ALK staining was not an exclusion criterion in the presence of an otherwise typical histologic appearance.

Among the 62 cases, the most common locations were lung (n=18), soft tissue (n=15), bladder (n=12), and gastrointestinal (GI) tract and liver (n=10). Less common sites included head and neck (n=4); adrenal and cervix, with one case each. One patient presented with disseminated lung, bone, liver disease.

ROS1 gene rearrangements identified in 10% of IMT most often in children

There were 6 *ROS1*-rearranged IMTs (Table 1), in two cases being associated with a *TFG* fusion (Fig. 1). There were 2 females and 4 males, with a mean age of 17.6 years (range 4-61). The anatomic locations included 2 in the lung, 3 intra-abdominal, and one in the esophagus. All except one patient occurred in children, with a mean of 9 years (range 4-18). Both *TFG-ROS1* fusion positive IMTs occurred in young children, an esophageal mass in a 4 year-old male and a pelvic tumor in a 4 year-old female. Morphologically, all pediatric tumors were composed of slender spindle cells with distinctive long cell processes arranged in loose fascicles, associated with mild to moderate inflammatory component and a variably fibromyxoid stroma (Fig. 1). The only non-pediatric IMT with *ROS1* gene rearrangement occurred in the omentum of a 61 year-old man and was composed of plump ovoid cells with marked inflammation (IMT3, Fig 1). All cases lacked significant cytologic atypia and showed low mitotic activity (1/10). All *ROS1*-rearranged IMTs were negative for ALK immunohistochemistry; in one case (IMT2) the tumor was additionally tested with the more sensitive D5F3 ALK antibody which was also negative. Immunohistochemical analysis for *ROS1* was performed in 4 cases showing diffuse positivity in 2 tumors (Fig. 1), patchy weak staining in one and negativity in the remaining case.

Novel RET rearrangement was identified in a pulmonary IMTs

The case occurred in a 27 year-old male with a 7.0 cm right upper lobe of lung mass, which was resected. Follow-up imaging 9 month later revealed a new 9.0 cm lesion in the left kidney which was proved to be metastatic. Patient succumbed of disease with widespread metastases 7 months later (IMT7, Table 1). The histology from both primary lung and kidney metastasis were reviewed and showed a solid pseudosarcomatous growth, with spindle cells arranged in 'herring-bone'-type fascicles. The tumor showed spindle cell morphology with mild to moderate nuclear atypia, and up to 4 MF/10 HPFs (Fig 2). The tumor showed immunopositivity for ALK (Fig 2).

EML4-ALK fusions occur with predilection in lung and soft tissue IMT

There were 35 cases (56%) with *ALK* gene rearrangement. The presence of *ALK* gene rearrangement correlated with positive ALK immunohistochemical staining, although in some cases the pattern of reactivity was patchy and weak. RNA sequencing was performed in 4 cases, two of them with *ALK* fusions (IMT8, IMT9) and two negative for all the probes tested (IMT46, IMT48). By Fusion seq, both *ALK*-rearranged tumors showed an *EML4-ALK* fusion candidate (Fig 3). This result was validated by RT-PCR in one case (Fig. 3) and by FISH for *EML4-ALK* fusion assay in both cases (Fig. 3). In the two remaining cases no fusion candidate was identified. An additional 5 *ALK*-rearranged IMTs were found to have an *EML4* fusion by screening the remaining *ALK*-positive IMTs by FISH (Table 2). The *EML4-ALK* fusion positive cases occurred in 6 females and one male, all except two presenting in children, including 2 newborns (range 0-39 years, mean 15). Most occurred in the lung (n= 5), with the remaining 2 in soft tissue (arm, omentum). The 2 IMT presenting in adult patients included a 36 year-old female (IMT12) with a tracheal lesion and a 39 year-old female with a lung lesion (IMT14). Morphologically, all 7 *EML4-ALK* fusion positive IMTs showed spindle cell morphology with low mitotic activity (1 MF/10 HPFs), mild to moderate inflammatory component and fibro-myxoid stroma. Two cases had an intermixed rhabdoid component (Fig. 4). Immunohistochemically, all except one case was positive for ALK (Table 2).

From the remaining 28 *ALK*-rearranged tumors, 7 occurred in the lung, 6 in the GI tract and liver, 5 in the bladder, 5 intra-abdominal, 3 trunk and mediastinum and 1 head and neck soft tissue (Supplementary Table 2). One patient presented with disseminated disease, involving lung, liver and bone. Although most of the *ALK*-rearranged lesions showed relatively typical morphology, with bland spindle cells, low mitotic activity, mild to moderate inflammation and fibromyxoid stroma, 2 cases showed distinctive epithelioid morphology, with high mitotic activity and focal marked nuclear pleomorphism (Fig. 5). In this group 3 (10%) cases were negative for ALK, while in the remaining 25 cases the presence of *ALK* gene abnormalities correlated with the ALK immunoreactivity.

Kinase Fusion-Negative IMTs Occur Predominantly in Adults

The remaining 20 cases lacked FISH abnormalities in all kinases tested, including *PDGFRB*, *NTRK1* and *LTK* (Supplementary Table 3 and see Discussion). There were 12 males and 8 females, with an age range of 9-72 years of age (mean 40). All except two patients were adults, range 20-74 years (mean 43). The only 2 pediatric cases occurred in the lung of a 9 year-old and in the adrenal gland of a 15 year-old. The anatomic distribution included bladder (n=7), lung (n=3), head and neck (n=3), GI and liver (n=3), soft tissue (n=2) and other sites one each (cervix, adrenal). In this group, most tumors (14/20, 70%) were negative for ALK immunoreactivity, (Supplementary Table 3).

Organ Site Associated Patterns of Kinase Fusions

Most pulmonary IMTs were positive for fusions (15/18 cases, 83%), either *ALK* (12 cases), *ROS1* (2 cases) or *RET* (1 case). Of the 12 *ALK*-rearranged lung IMTs, 5 (42%) showed the *EML4-ALK* fusions. In fact most *EML4-ALK* fusion positive IMTs occurred in the lung, 5/7

(71%) cases. Less than half (42%) of the bladder IMT showed *ALK* kinase fusions, with most of the cases (83%) being diagnosed in adults.

All except one of the H&N IMT lacked fusions in any of the kinases investigated suggesting alternative pathogenesis. Interestingly most of the fusion negative IMTs were adults (18/20, 90%) and the prevalent site was the bladder (n=7). Compared to the *ALK* and *ROS1* rearranged tumors, the fusion negative IMT showed an under-representation of lung and soft tissue sites, and over-representation of the head and neck.

DISCUSSION

Inflammatory myofibroblastic tumor (IMT) is currently classified as an intermediate, rarely metastasizing neoplasm composed of myofibroblasts accompanied by an inflammatory infiltrate of plasma cells, variable lymphocytes, and eosinophils¹. Most patients with IMT are children, adolescents, or young adults, although the tumor can occur throughout life. IMT can occur anywhere in the body, but has a predilection for the abdominal cavity, lung, and bladder^{10, 22}. Approximately 50–70% of the tumors harbor an *Anaplastic Lymphoma Kinase (ALK)* gene rearrangement, leading to the formation of a chimeric fusion protein, which is detectable by immunohistochemistry or FISH^{2, 10}. *ALK* expression and/or *ALK* gene rearrangement was previously described as a good prognostic marker in IMT, with positive cases showing a better outcome, while *ALK*-negative IMTs being more aggressive with a higher frequency of metastasis compared with *ALK*-positive IMT^{9,10}. However, it is possible that *ALK*-negative tumors represent either IMT with different genetic abnormalities or different entities all together.

Anaplastic lymphoma kinase (*ALK*) is a receptor-type protein tyrosine kinase that is currently the focus of much attention in oncology. *ALK* is rendered oncogenic as a result of its fusion to many gene partners, more commonly to *NPM* in anaplastic large cell lymphoma²³, to *TPM3* or *TPM4* in IMT³, to *EML4* in non-small cell lung carcinoma (NSCLC)²⁴, and to *VCL* in renal medullary carcinoma²⁵⁻²⁷. It is also activated as a result of missense mutations in neuroblastoma²⁸ and anaplastic thyroid cancer²⁹. The term “*ALKoma*” was suggested in order to unify these various tumors arising in different organs but sharing oncogenic *ALK* activation as an essential growth driver, which defines their potential susceptibility to *ALK* inhibitors³⁰. One of such compounds, crizotinib, is now approved in the United States for the treatment of lung cancer positive for *ALK* rearrangement.

ALK fusions similar to other translocations that activate receptor TKs bind their catalytic domain to strongly or ubiquitously expressed proteins with dimerization or oligomerization domains. In anaplastic large cell lymphoma, *NPM* (nucleophosmin) provides both a strong constitutive promoter and an oligomerization domain³¹. Similarly, the *TPM3/4* tropomyosin proteins include the coiled coil dimerization domain in the fusion, suggesting a similar role as dimerization partners within these fusions³. In IMT, more than 10 different genes have been identified as *ALK* fusion partners, including *TPM3/4*, *RANBP2*, *TFG*, *CARS*, *ATIC*, *LMNA*, *PRKAR1A*, *CLTC*, *FN1*, *SEC31A*, *EML4*¹²³². Due to this significant molecular heterogeneity and the fact that most *ALK* gene partners have similar functions in providing a

strong promoter and an oligomerization domain, resulting in oncogenic activation of the ALK kinase, our study focused on identifying rearrangements of a large panel of actionable kinases, rather than catalogue their ubiquitous partners.

EML4 and *ALK* genes are mapped to the short arm of chromosome 2 in opposite orientations, thus a small inversion *inv2(2)(p21p23)* is required to give rise to a functional *EML4-ALK* fusion-type tyrosine kinase²⁴. *EML4-ALK* was initially described only in NSCLC, however, a case report recently identified this abnormality in a pulmonary IMT in a 67 year-old man³³. Subsequently, in the series by Lovly et al, 2 additional *EML4-ALK* fusion positive IMTs were identified by RNAseq both in the lung¹². Our study provides further evidence for *EML4-ALK* being involved in the pathogenesis of IMT, which is present in about 20% of the *ALK*-rearranged IMTs studied. We report this gene fusion abnormality in 7 cases, 5 of them occurring in the lung and 2 in the soft tissue, the latter a previously unreported finding. These results suggest that identical *EML4-ALK* present in different tumor types may drive an inappropriate activation of the same kinase signaling pathway which could be oncogenic in disparate cellular lineages. Both transgenic and CRISPR/Cas murine models expressing *EML4-ALK4* in lung epithelial cells were described as resulting in NSCLC phenotype and being responsive to ALK inhibitors^{34, 35}. None of these genetic models result in an IMT phenotype, suggesting that the transformed cell of origin, i.e. lung epithelium, is critical in dictating the phenotype, specifically NSCLC.

ALK receptor tyrosine kinase belongs to the insulin receptor family and is most closely related to leukocyte tyrosine kinase (LTK) with which it shows 79% amino acid identity in the kinase domain and extensive homology elsewhere³⁶. As such we have tested the kinase-negative IMT in this series for potential *LTK* gene abnormalities by FISH, however, none were detected, suggesting that this RTK is not involved in the pathogenesis of IMT.

A recent study pointed out that IMTs harbor additional actionable targets, such as *ROS1* and in one case *PDGFRB* fusions¹². This study applying RNA sequencing found that the majority of IMTs (85%) displayed kinase fusions. Notably, *ALK* fusions were detected in 2 of 11 IMT samples that tested negative for ALK expression by IHC, underlying the risk of denying therapy with an ALK inhibitor based on IHC alone. Our study further emphasizes this caveat, with lack of ALK immunorexpression in 24% (10/42) of fusion positive IMTs, including all *ROS1*-rearranged cases and 4/35 (11%) of *ALK*-rearranged IMTs. It remains to be determined by larger studies if the more sensitive ALK monoclonal antibody, D5F3, is more reliable in identifying *ALK*-gene rearrangements than the ALK01, since they had overlapping results in the 3 cases tested. Similar observations were noted with *ROS1* IHC, with only 3 of the 4 *ROS1*-rearranged tumors showing positive staining, including one strong and diffuse and the other two cases relatively patchy and weak. In our opinion FISH testing should be performed in IMT with typical morphologic features but negative ALK immunostaining, especially in recurrent/advanced lesions in which systemic therapy with kinase inhibitors could be beneficial.

In the study by Lovly et al, 3 IMT patients with *ROS1*-related fusions are described, involving soft tissue in 2 cases and lung in one¹². As *TFG-ROS1* fusions were identified in 2 of the 3 tumors, we have also investigated this specific fusion in our cohort, and found that

half of the cases showed similar fusion. Among our 6 *ROS1*-rearranged IMTs, we see a similar anatomic distribution, with 3 in soft tissue, 2 in lung and one in the GI tract (esophagus). In our series all except one tumor occurred in pediatric patients and showed a bland morphologic appearance with spindle cells showing slender and long cell processes.

Our study also describes novel *RET* gene rearrangement in a patient with pulmonary IMT, which was associated with a fatal clinical outcome. *RET* fusions have been described in NSCLC, typically in younger patients, never smokers and in early tumor stages^{37,38}. Histologically, *RET* and *ROS1* fusion positive NSCLC share the solid signet-ring cell and mucinous cribriform pattern, seen with *ALK* fusion positive NSCLC³⁹. *RET* and *ROS1* fusion positive comprise about 1% of lung adenocarcinomas, while *ALK* rearrangements are seen in 5% of cases⁴⁰.

Despite a comprehensive screening for kinase fusions, both our and Lovly et al¹² studies identified abnormalities in most but not all IMT cases. In our series, 6/20 (30%) fusion negative IMTs showed *ALK* immunoreactivity, suggesting alternative mechanisms of *ALK* activation. However, most IMTs lacking kinase rearrangements were negative for *ALK* protein expression, raising the possibility of alternative diagnosis. In the bladder cohort, some of the *ALK*-negative IMTs with bland morphology could represent post-operative spindle cell nodules or other pseudosarcomatous myofibroblastic proliferations⁴¹.

In summary, our study investigated genetic abnormalities across a large panel of actionable kinases by combined FISH and RNA sequencing methodology in a diverse clinical and pathologic spectrum of IMTs. As recently reported, our results confirm that two-thirds of IMT show *ALK* and *ROS1* related fusions. Our findings also identify a rare case with novel *RET* gene rearrangement, occurring in a lung IMT. These results further reveal interesting correlations between genotype and clinical presentation in IMT. Most pulmonary IMTs (83%) were positive for fusions, either *ALK* or *ROS1*. In fact most *EML4-ALK* fusion positive IMTs (71%) occurred in the lung, with the remaining cases occurring in the soft tissue. Among the 23 pediatric IMTs studied all except 2 cases (91%) were positive for kinase fusions, while in contrast, most of the fusion negative IMTs (90%) occurred in adults and rarely arose in lung or soft tissue. These data not only provide insight into this rare tumor type but also offer rational targeted therapeutic strategies with existing FDA-approved TKIs based on the genomic profile of the tumor.

Supplementary Material

Refer to Web version on PubMed Central for supplementary material.

Acknowledgments

Supported in part by: P50 CA 140146-01 (CRA), Cycle for Survival (CRA)

REFERENCES

1. Fletcher, C.; Bridge, JA.; Hogendoorn, PC., et al. WHO Classification of Tumours of Soft Tissue and Bone. IARC; Lyon: 2013.

2. Griffin CA, Hawkins AL, Dvorak C, et al. Recurrent involvement of 2p23 in inflammatory myofibroblastic tumors. *Cancer Res.* 1999; 59:2776–2780. [PubMed: 10383129]
3. Lawrence B, Perez-Atayde A, Hibbard MK, et al. TPM3-ALK and TPM4-ALK oncogenes in inflammatory myofibroblastic tumors. *Am J Pathol.* 2000; 157:377–384. [PubMed: 10934142]
4. Bridge JA, Kanamori M, Ma Z, et al. Fusion of the ALK gene to the clathrin heavy chain gene, CLTC, in inflammatory myofibroblastic tumor. *Am J Pathol.* 2001; 159:411–415. [PubMed: 11485898]
5. Cools J, Wlodarska I, Somers R, et al. Identification of novel fusion partners of ALK, the anaplastic lymphoma kinase, in anaplastic large-cell lymphoma and inflammatory myofibroblastic tumor. *Genes Chromosomes Cancer.* 2002; 34:354–362. [PubMed: 12112524]
6. Saab ST, Hornick JL, Fletcher CD, et al. IgG4 plasma cells in inflammatory myofibroblastic tumor: inflammatory marker or pathogenic link? *Mod Pathol.* 2011; 24:606–612. [PubMed: 21297584]
7. Vaglio A, Salvarani C, Buzio C. Retroperitoneal fibrosis. *Lancet.* 2006; 367:241–251. [PubMed: 16427494]
8. Coffin CM, Patel A, Perkins S, et al. ALK1 and p80 expression and chromosomal rearrangements involving 2p23 in inflammatory myofibroblastic tumor. *Mod Pathol.* 2001; 14:569–576. [PubMed: 11406658]
9. Chan JK, Cheuk W, Shimizu M. Anaplastic lymphoma kinase expression in inflammatory pseudotumors. *Am J Surg Pathol.* 2001; 25:761–768. [PubMed: 11395553]
10. Coffin CM, Hornick JL, Fletcher CD. Inflammatory myofibroblastic tumor: comparison of clinicopathologic, histologic, and immunohistochemical features including ALK expression in atypical and aggressive cases. *Am J Surg Pathol.* 2007; 31:509–520. [PubMed: 17414097]
11. Marino-Enriquez A, Wang WL, Roy A, et al. Epithelioid inflammatory myofibroblastic sarcoma: An aggressive intra-abdominal variant of inflammatory myofibroblastic tumor with nuclear membrane or perinuclear ALK. *Am J Surg Pathol.* 2011; 35:135–144. [PubMed: 21164297]
12. Lovly CM, Gupta A, Lipson D, et al. Inflammatory myofibroblastic tumors harbor multiple potentially actionable kinase fusions. *Cancer Discovery.* 2014; 4:889–895. [PubMed: 24875859]
13. Antonescu CR, Zhang L, Chang NE, et al. EWSR1-POU5F1 fusion in soft tissue myoepithelial tumors. A molecular analysis of sixty-six cases, including soft tissue, bone, and visceral lesions, showing common involvement of the EWSR1 gene. *Genes Chromosomes Cancer.* 2010; 49:1114–1124. [PubMed: 20815032]
14. Quail MA, Kozarewa I, Smith F, et al. A large genome center's improvements to the Illumina sequencing system. *Nature Methods.* 2008; 5:1005–1010. [PubMed: 19034268]
15. Hsu F, Kent WJ, Clawson H, et al. The UCSC Known Genes. *Bioinformatics.* 2006; 22:1036–1046. [PubMed: 16500937]
16. Habegger L, Sboner A, Gianoulis TA, et al. RSEQtools: a modular framework to analyze RNA-Seq data using compact, anonymized data summaries. *Bioinformatics.* 2011; 27:281–283. [PubMed: 21134889]
17. Sboner A, Habegger L, Pflueger D, et al. FusionSeq: a modular framework for finding gene fusions by analyzing paired-end RNA-sequencing data. *Genome Biology.* 2010; 11:R104. [PubMed: 20964841]
18. Tanas MR, Sboner A, Oliveira AM, et al. Identification of a disease-defining gene fusion in epithelioid hemangioendothelioma. *Science Translational Medicine.* 2011; 3:98ra82.
19. Pierron G, Tirode F, Lucchesi C, et al. A new subtype of bone sarcoma defined by BCORCCNB3 gene fusion. *Nat Genet.* 2012; 44:461–466. [PubMed: 22387997]
20. Mosquera JM, Sboner A, Zhang L, et al. Recurrent NCOA2 gene rearrangements in congenital/infantile spindle cell rhabdomyosarcoma. *Genes Chromosomes Cancer.* 2013; 52:538–550. [PubMed: 23463663]
21. Sanders HR, Li HR, Bruey JM, et al. Exon scanning by reverse transcriptase-polymerase chain reaction for detection of known and novel EML4-ALK fusion variants in non-small cell lung cancer. *Cancer Genetics.* 2011; 204:45–52. [PubMed: 21356191]
22. Coffin CM, Watterson J, Priest JR, et al. Extrapulmonary inflammatory myofibroblastic tumor (inflammatory pseudotumor). A clinicopathologic and immunohistochemical study of 84 cases. *Am J Surg Pathol.* 1995; 19:859–872. [PubMed: 7611533]

23. Morris SW, Kirstein MN, Valentine MB, et al. Fusion of a kinase gene, ALK, to a nucleolar protein gene, NPM, in non-Hodgkin's lymphoma. *Science*. 1994; 263:1281–1284. [PubMed: 8122112]
24. Soda M, Choi YL, Enomoto M, et al. Identification of the transforming EML4-ALK fusion gene in non-small-cell lung cancer. *Nature*. 2007; 448:561–566. [PubMed: 17625570]
25. Smith NE, Deyrup AT, Marino-Enriquez A, et al. VCL-ALK renal cell carcinoma in children with sickle-cell trait: the eighth sickle-cell nephropathy? *Am J Surg Pathol*. 2014; 38:858–863. [PubMed: 24698962]
26. Debelenko LV, Raimondi SC, Daw N, et al. Renal cell carcinoma with novel VCL-ALK fusion: new representative of ALK-associated tumor spectrum. *Mod Pathol*. 2011; 24:430–442. [PubMed: 21076462]
27. Marino-Enriquez A, Ou WB, Weldon CB, et al. ALK rearrangement in sickle cell trait-associated renal medullary carcinoma. *Genes Chromosomes Cancer*. 2011; 50:146–153. [PubMed: 21213368]
28. George RE, Sanda T, Hanna M, et al. Activating mutations in ALK provide a therapeutic target in neuroblastoma. *Nature*. 2008; 455:975–978. [PubMed: 18923525]
29. Murugan AK, Xing M. Anaplastic thyroid cancers harbor novel oncogenic mutations of the ALK gene. *Cancer Res*. 2011; 71:4403–4411. [PubMed: 21596819]
30. Mano H. ALKoma: a cancer subtype with a shared target. *Cancer Discovery*. 2012; 2:495–502. [PubMed: 22614325]
31. Bischof D, Pulford K, Mason DY, et al. Role of the nucleophosmin (NPM) portion of the non-Hodgkin's lymphoma-associated NPM-anaplastic lymphoma kinase fusion protein in oncogenesis. *Mol Cell Biol*. 1997; 17:2312–2325. [PubMed: 9121481]
32. Debelenko LV, Arthur DC, Pack SD, et al. Identification of CARS-ALK fusion in primary and metastatic lesions of an inflammatory myofibroblastic tumor. *Laboratory Investigation; a journal of technical methods and pathology*. 2003; 83:1255–1265.
33. Sokai A, Enaka M, Sokai R, et al. Pulmonary inflammatory myofibroblastic tumor harboring EML4-ALK fusion gene. *Japanese Journal of Clinical Oncology*. 2014; 44:93–96. [PubMed: 24277751]
34. Soda M, Takada S, Takeuchi K, et al. A mouse model for EML4-ALK-positive lung cancer. *Proc Natl Acad Sci U S A*. 2008; 105:19893–19897. [PubMed: 19064915]
35. Maddalo D, Manchado E, Concepcion CP, et al. In vivo engineering of oncogenic chromosomal rearrangements with the CRISPR/Cas9 system. *Nature*. 2014
36. Morris SW, Naeve C, Mathew P, et al. ALK, the chromosome 2 gene locus altered by the t(2;5) in non-Hodgkin's lymphoma, encodes a novel neural receptor tyrosine kinase that is highly related to leukocyte tyrosine kinase (LTK). *Oncogene*. 1997; 14:2175–2188. [PubMed: 9174053]
37. Takeuchi K, Soda M, Togashi Y, et al. RET, ROS1 and ALK fusions in lung cancer. *Nature Medicine*. 2012; 18:378–381.
38. Kohno T, Ichikawa H, Totoki Y, et al. KIF5B-RET fusions in lung adenocarcinoma. *Nature Medicine*. 2012; 18:375–377.
39. Lee SE, Lee B, Hong M, et al. Comprehensive analysis of RET and ROS1 rearrangement in lung adenocarcinoma. *Mod Pathol*. 2014
40. Pan Y, Zhang Y, Li Y, et al. ALK, ROS1 and RET fusions in 1139 lung adenocarcinomas: a comprehensive study of common and fusion pattern-specific clinicopathologic, histologic and cytologic features. *Lung Cancer*. 2014; 84:121–126. [PubMed: 24629636]
41. Hirsch MS, Dal Cin P, Fletcher CD. ALK expression in pseudosarcomatous myofibroblastic proliferations of the genitourinary tract. *Histopathology*. 2006; 48:569–578. [PubMed: 16623783]

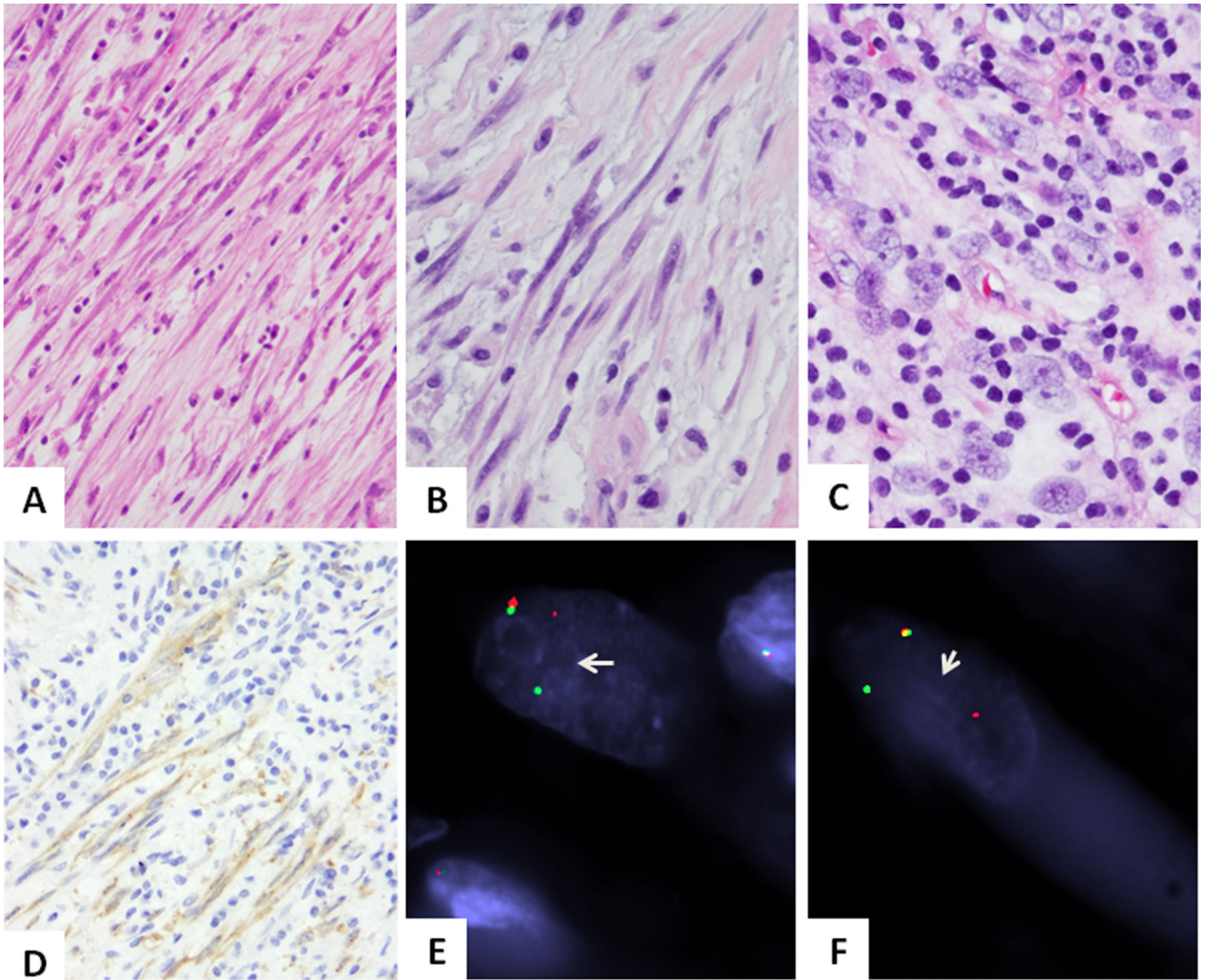


Figure 1. Pathologic findings of ROS1-rearranged IMTs

Most cases showed a distinctive spindle cell proliferation with long, slender cell processes, within a loose edematous stroma with scant inflammatory component (**A**. IMT6, 200x, **B**. IMT2, 400x). The only adult IMT case in this genomic group showed more plump cells with ill-defined cell borders, vesicular chromatin and distinctive nucleoli and more abundant lymphocytic inflammatory infiltrate (**C**. IMT3, 400x). ROS1 immunostaining highlights the long cell processes of lesional cells (**D**. IMT2, 200x). FISH showing balanced *ROS1* (**E**) and *TFG* (**F**) break-apart signals (arrows; IMT6; red, centromeric; green, telomeric).

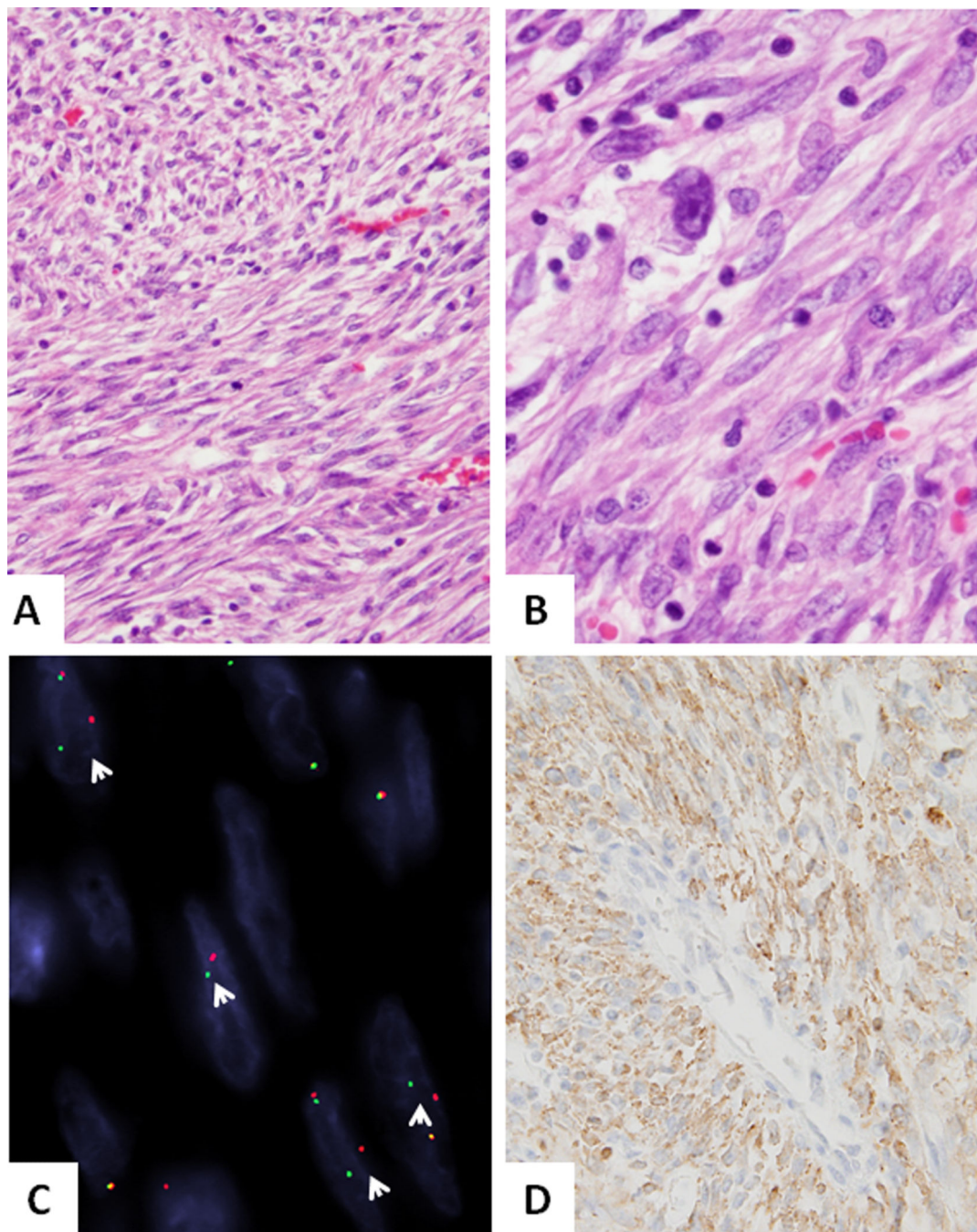


Figure 2. Novel RET-rearrangement in a pulmonary IMT (IMT7)

(A,B) A compact proliferation of relatively monotonous spindle cells arranged in intersecting long fascicles, with scant intervening stroma and mild inflammation (200x). Higher power depicts scattered pleomorphic cells with enlarged nuclei and prominent nucleoli (400x). C. FISH assay showing break-apart signals consistent with RET gene rearrangement (arrows, red centromeric, green, telomeric). D. ALK immunohistochemistry showing diffuse reactivity.

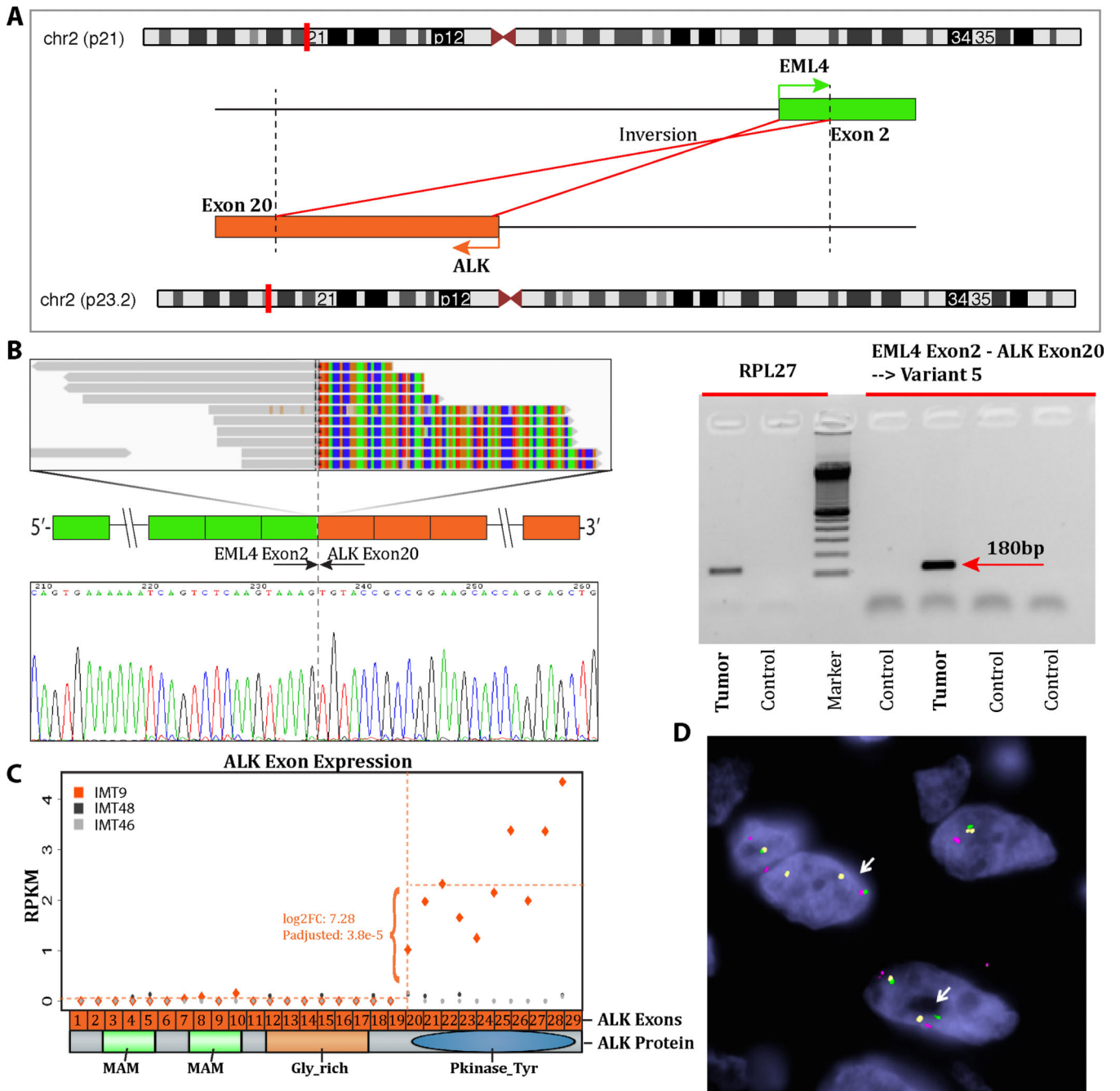


Figure 3. RNAseq and Fusion Seq discovery of *EML4-ALK* and experimental validation (IMT8-9)

A. Schematic representation of the fusion transcript candidate identified by RNAseq, involving the *EML4* locus on 2p21 with *ALK* located on 2p23.2, resulting in an inv(2) (p21p23) inversion. **B.** RT-PCR validation and ABI sequence showing that *EML4* exon 4 is fused to *ALK* exon 20, as previously described (IMT8)³⁷. **C.** Upregulated expression of the 3' portion of *ALK* mRNA starting with exon 20, which is included in the fusion (IMT9). Diagrammatic representation of *ALK* domains, with the entire kinase domain being preserved in the predicted fusion protein. **D.** FISH fusion assay showing *ALK* (red,

centromeric) fused to centromeric portion of EML4 (green); away from the telomeric part of EML4, labeled in yellow (IMT9, arrows).

Author Manuscript

Author Manuscript

Author Manuscript

Author Manuscript

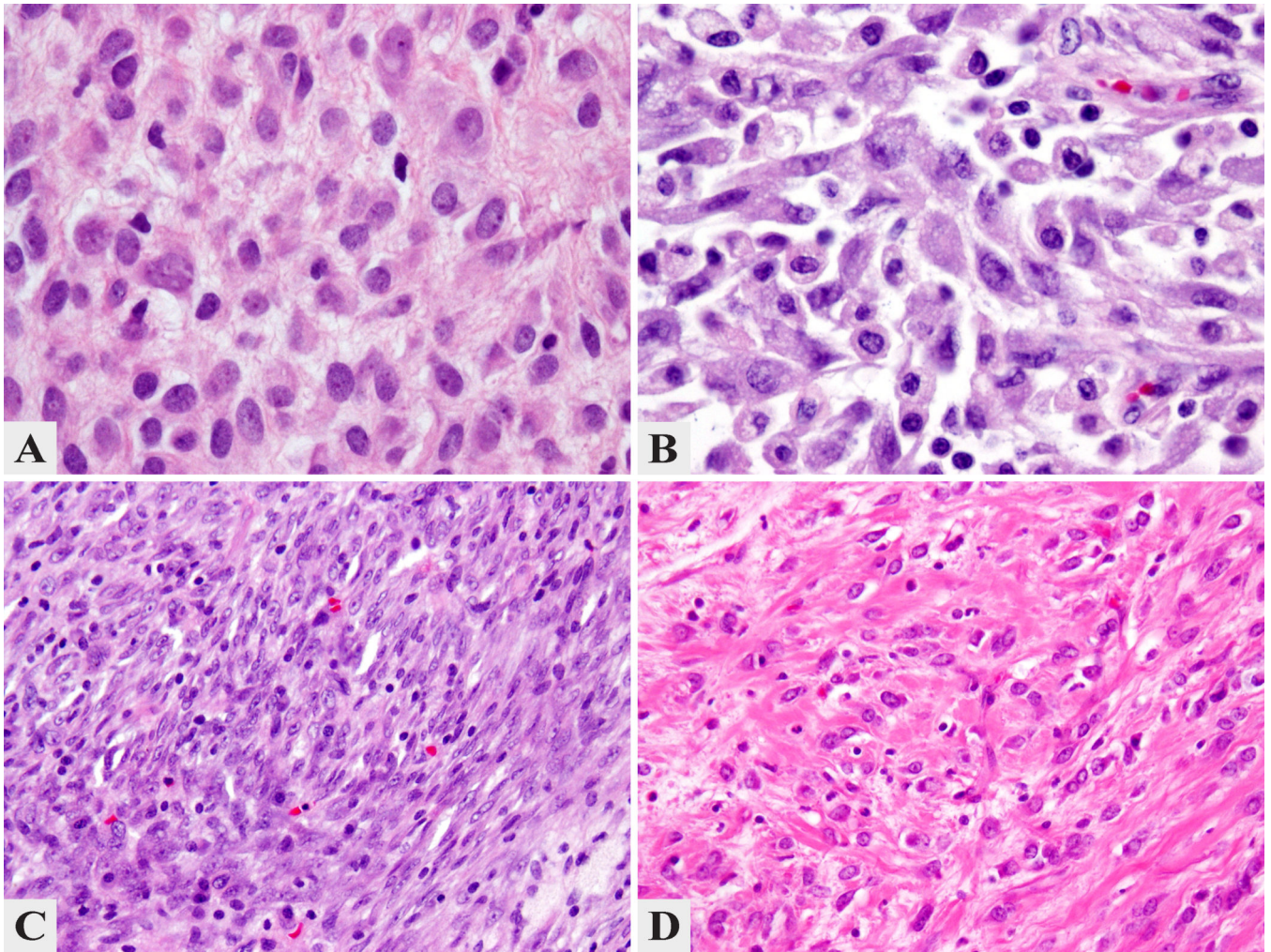


Figure 4. Morphologic Features of *EML4-ALK* Fusion Positive IMTs

The 2 index cases studied by RNAseq showing epithelioid to rhabdoid-like cells with light eosinophilic to amphophilic cytoplasm, within a loose stroma with scant inflammatory infiltrate (**A**. IMT8 and **B**. IMT9 ; 400x). The tracheal IMT from a 36 year-old female (**C**. IMT12, 200x) revealed a compact growth of monotonous spindle cells, while the omental IMT from a newborn girl showed a more prominent fibrous stromal component (**D**. IMT11, 200x).

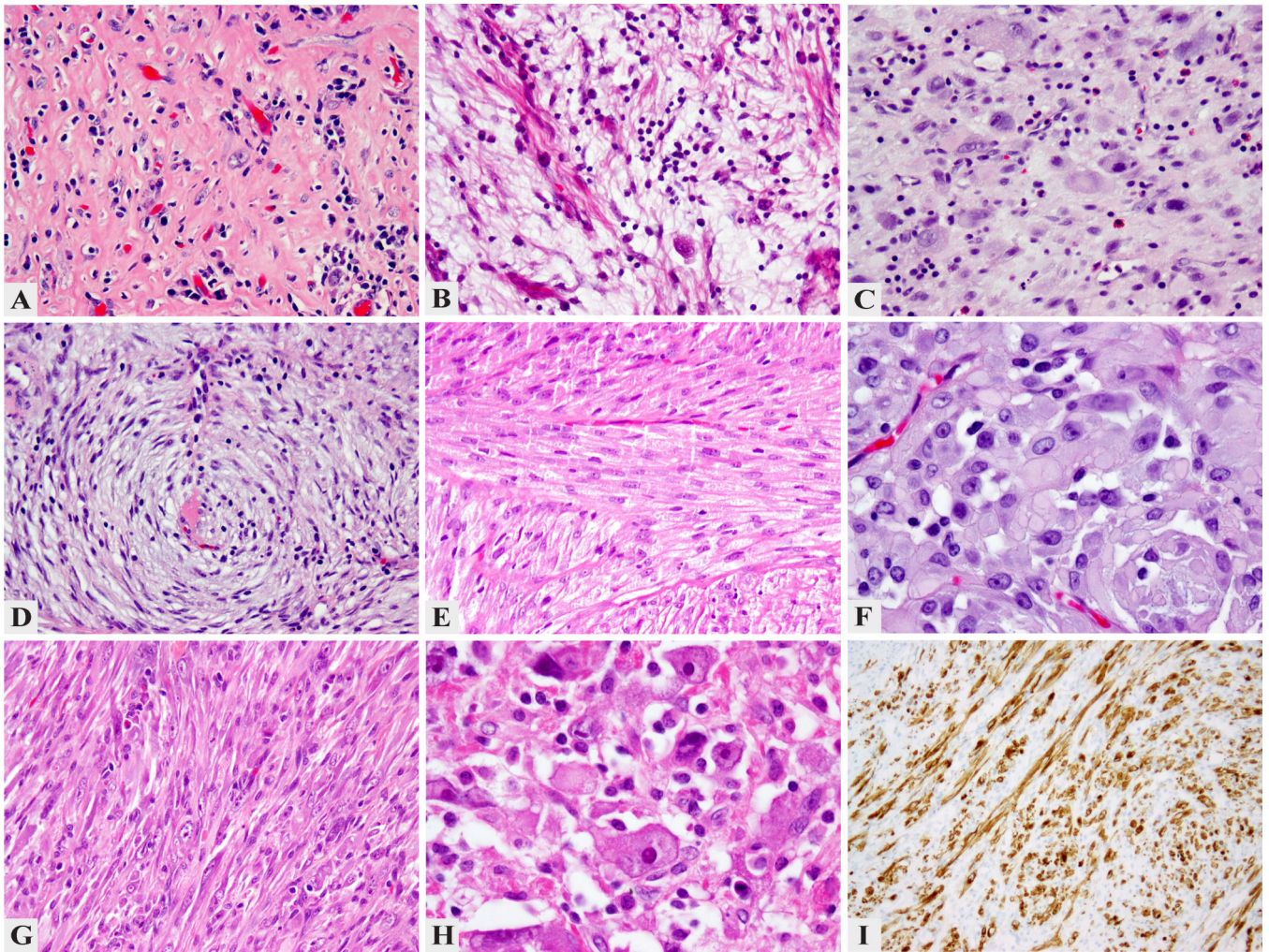


Figure 5. Morphologic Spectrum of ALK-Rearranged IMTs

Despite shared ALK gene abnormalities, there was a significant variability in histologic appearance, including: prominent hyalinization and inflammation with only rare lesional cells (A. IMT36, 200x); abundant myxoid stroma and moderate degree of inflammation with scattered spindle cells (B. IMT29, 200x); enlarged histiocytoid cells separated by conspicuous edematous stroma with numerous eosinophils, reminiscent of Hodgkin's lymphoma (C. IMT25, 200x); spindle cell morphology with a distinctive whorling pattern and scant inflammation (D. IMT37, 200x); solid fascicular growth of monotonous spindle cell with eosinophilic cytoplasm reminiscent of a smooth muscle neoplasm (E. IMT21, 200x); distinctive epithelioid morphology, arranged in vague nests (F. IMT39, 400x); pseudosarcomatous growth with some cells showing enlarged vesicular nuclei with prominent nucleoli (G. IMT28, 200x); pleomorphic phenotype with rhabdoid like cells showing large open nuclei with virocyte-like inclusions (H. IMT24, 400x); strong ALK immunohistochemistry in a bladder IMT (I. IMT23, 200x).

Table 1Clinical, Immunohistochemical and FISH Findings in *ROS1* and RET-rearranged IMTs

| IMT | Age/Sex | Location | ROS1 / TFG /RET FISH results | Histologic Findings, MF/10HPFs | ROS1 IHC | ALK IHC |
|-----|---------|-----------------|------------------------------|--|----------|---------|
| 1 | 18/M | lung | ROS1 Pos / TFG Neg | Spindle cells, fascicles, no atypia, 1/10 | Neg | Neg |
| 2 | 7/M | lung | ROS1 Pos / TFG Neg | Spindle cells, fascicles, no atypia, 1/10 | Pos | Neg* |
| 3 | 61/M | intra-abdominal | ROS1 Pos / TFG Neg | Plump ovoid cells with prominent inflammation, 1/10 | ND | Neg |
| 4 | 12/F | intra-abdominal | ROS1 Pos / TFG Neg | Spindle cells, tissue culture-like growth, mild atypia, 1/10 | ND | Neg |
| 5 | 4/M | esophagus | ROS1 Pos / TFG Pos | Spindle cells, fascicles, no atypia, 1/10 | Pos | Neg |
| 6 | 4/F | pelvis | ROS1 Pos / TFG Pos | Spindle cells, fascicles, no atypia, 1/10 | Pos | Neg |
| 7 | 27/M | lung | RET Pos | Spindle cells, 'herring-bone' fascicles, mild atypia, 4/10 | ND | Pos |

F, female; M, male

* IHC done with 2 ALK antibodies: ALK01 (Ventana ready to use) and D5F3 (Cell Signaling; 1:50); pos, positive; neg, negative; ND, not done; MF/10HPFs, mitotic figures/ 10 high power fields

Table 2Clinical and Pathologic Features of *EML4-ALK* Fusion positive IMTs

| IMT | Age/Sex | Location | Cellular morphology, MF/HPFs | ALK IHC |
|-----|---------|----------|--|---------|
| 8* | 6mo/F | Arm | Plump spindle to rhabdoid cells, 1/10 | Pos |
| 9* | 6/F | Lung | Plump spindle, rare rhabdoid cells, 1/10 | Pos |
| 10 | 5/M | Lung | Spindle cells, 1/10 | Pos |
| 11# | NB | Omentum | Spindle cells, 1/10 | Pos |
| 12 | 36/F | Trachea | Spindle cells, 1/10 | Pos |
| 13 | 18/F | Lung | Spindle cells, 1/10 | Neg |
| 14 | 39/F | Lung | Spindle cells, 1/10 | Pos |

* confirmed by RNAseq

dot-like IHC pattern of ALK staining; Mo, months; NB, new-born, F, female; M, male; Pos, positive; neg, negative, MF/10 HPFs; mitotic figures/10 high power fields.